Polarized Light Scattering Spectroscopy for Quantitative Measurement of Epithelial Cellular Structures *In Situ*

Vadim Backman, Rajan Gurjar, Kamran Badizadegan, Irving Itzkan, Ramachandra R. Dasari, Lev T. Perelman, and Michael S. Feld

***Abstract*—We report an *in situ* method of probing the structure of living epithelial cells, based on light scattering spectroscopy with polarized light. The method makes it possible to distinguish between single backscattering from uppermost epithelial cells and multiply scattered light. The spectrum of the single backscattering component can be further analyzed to provide histological information about the epithelial cells such as the size distribution of the cell nuclei and their refractive index. These are valuable quantities to detect and diagnose precancerous changes in human tissues.**

***Index Terms*—Cancer diagnosis, light scattering, medical spectroscopy, polarization.**

I. Introduction

CHARACTERIZATION of cellular structures in living systems is an important problem in biomedical science. The ability to extract quantitative information in living cells *in situ* without perturbing them, could be used to study biophysical processes in living systems and to monitor morphological and physiological changes such as precancerous or cancerous conditions. At present, such information can only be obtained by tissue removal or scraping. Currently, techniques such as microscopy and flow cytometry are used to probe intracellular structure, and applying them *in situ* is not possible. In this paper we present an *in situ* method of probing the structure of living cells, based on light scattering spectroscopy (LSS) with polarized light.

Body surfaces are lined by a cohesive and richly cellular epithelial layer, which in association with the underlying supporting structures form a mucosal lining. Light traversing the epithelial layer can be scattered by cell organelles of various sizes, such as mitochondria and nuclei, which have refractive indices higher than that of the surrounding cytoplasm [1]. The cell nuclei are appreciably larger than the optical wavelength (typically 5–10 μm versus 0.5 μm). They predominantly scatter light in the forward direction, and there is appreciable scattering in the backward direction, as well [2].

Manuscript received February 16, 1999; revised May 28, 1999. This work was supported by the NIH under Grant P41-RR02594 and Grant R01-CA53717.

V. Backman, R. Gurjar, I. Itzkan, R. R. Dasari, L. T. Perelman, and M. S. Feld are with G. R. Harrison Spectroscopy Laboratory, Massachusetts Institute of Technology, Cambridge, MA 02139 USA.

K. Badizadegan is with the Department of Pathology, Children's Hospital, Boston, MA 02115 USA.

Publisher Item Identifier S 1077-260X(99)07526-7.

We have previously shown that the backscattered light has a wavelength-dependent oscillatory component [3]. The periodicity of this component increases with nuclear size, and its amplitude is related to cellularity or the population density of the epithelial nuclei. By analyzing the frequency and amplitude of this oscillatory component, the size distribution and density of epithelial nuclei can be extracted. However, the measurements reported in [3] used unpolarized light, and in order to extract the information of interest, it was necessary to use a physical model to remove the large background from underlying tissue. In this paper, we discuss the use of polarized light in LSS, and show that it provides a direct experimental method for background removal, as well as other advantages.

One important application of a technique capable of measuring quantitative changes of intracellular structures *in situ* is early diagnosis of cancer or precancerous lesions. More than 90% of all cancers are epithelial in origin [4]. Most epithelial cancers have a well-defined precancerous stage characterized by nuclear atypia and dysplasia. Lesions detected at this stage can potentially be eradicated with early diagnosis. However, many forms of atypia and dysplasia are flat and not visually observable. Thus, surveillance for invisible dysplasia employs random biopsy, followed by microscopic examination of the biopsy material by a pathologist. However, usually only a small fraction of the epithelial surface at risk for dysplasia can be sampled in this way, potentially resulting in a high sampling error.

The various forms of epithelial dysplasia exhibit some common morphological changes on microscopic examination, the most prominent of which relate to the nuclear morphology. The nuclei become enlarged, pleomorphic (irregular in contour and size distribution), "crowded" (they occupy more of the tissue volume), and hyperchromatic (they stain more intensely with nuclear stains) [5]. Light-scattering spectroscopy is capable of providing quantitative information to characterize these features and, as a noninvasive optical technique, it is well suited for use in dysplasia surveillance [6]. LSS can be applied *in situ* does not require tissue removal, and analysis can be performed in real time.

However, in applying LSS to human tissues, one has to overcome the problem of removing the large contribution to the reflected light caused by diffuse scattering from underlying tissue layers. To better understand this problem, consider the architecture of the superficial tissues of the body. Body

surfaces are covered with a thin layer of epithelial tissue. The thickness of the epithelium in various organs ranges from less than 10 μm in simple (single layer) squamous epithelia to several hundred μm in stratified (multiple cell layers) epithelia. Beneath all epithelia are variable layers of the supporting components including relatively hypocellular connective tissues, inflammatory cells, and neurovascular structures. In order to detect changes in epithelial cell nuclei associated with dysplasia, one must differentiate the light reflected from the epithelial layer from that of the underlying tissue. Since the penetration depth in tissue substantially exceeds the epithelial thickness, the backscattered light from epithelial nuclei is ordinarily very small in amplitude, and it is easily masked by the diffuse background from the underlying tissue. To analyze the backscattered component, this background must be removed. Previously, this was accomplished by modeling the general spectral features of the background [3]. However, this approach must be specifically adapted to each different type of tissue studied, and its accuracy is theory dependent. To optimize the use of LSS for various medical applications, it is of interest to consider more robust methods of removing or significantly reducing the diffuse component of the scattered light.

This paper reports an experimental means of isolating the scattering from epithelial cell nuclei using polarized light. It is well known that initially polarized light looses its polarization when traversing a turbid medium [7], [8] such as biological tissue [9]. In contrast, the polarization of the light scattered backward after a single scattering event is preserved. This property of polarized light has been used to image surface and near surface biological tissues [10]. Thus, by subtracting off the unpolarized component of the scattered light, the contribution due to backscattering from epithelial cell nuclei can be readily distinguished. The residual spectrum can be further analyzed to extract the size distribution of the nuclei, their population density, and their relative refractive index.

II. Theoretical Model

Mie theory provides an exact analytical expression for the scattering of a plane wave of wave number k by a sphere of diameter d and relative refractive index n. For a plane wave incident in direction $\hat{\boldsymbol{s}}_0$, light scattered into direction $\hat{\boldsymbol{s}}$ will have components that are polarized parallel (p) and perpendicular (s) to the plane of scattering. The intensities I_p and I_s of these respective components are related to the corresponding intensities of the incident light as follows:

$$I_p(\hat{\boldsymbol{s}}) = \frac{|S_2(\hat{\boldsymbol{s}},\hat{\boldsymbol{s}}_0)|^2}{k^2r^2} I_p^0(\hat{\boldsymbol{s}})_0 \tag{1}$$

$$I_s(\hat{\boldsymbol{s}}) = \frac{|S_1(\hat{\boldsymbol{s}},\hat{\boldsymbol{s}}_0)|^2}{k^2r^2} I_s^0(\hat{\boldsymbol{s}}_0) \tag{2}$$

with r the distance from the scatterer to the detector. The scattering amplitudes S_1 and S_2 can be calculated numerically using Mie theory [11]. They are functions of the scattering angle $\vartheta = \cos^{-1}(\hat{\boldsymbol{s}}\cdot\hat{\boldsymbol{s}}_0)$, and are normalized such that integral $(\pi/k^2)\int_0^\pi (|S_1(\vartheta)|^2 + |S_2(\vartheta)|^2)\sin\vartheta\, d\vartheta$ is equal to the total elastic scattering cross section.

Now consider an experiment in which linearly polarized incident light, intensity I_0, is distributed over solid angle $\Delta\Omega_0$ and scattering is collected over solid angle $\Delta\Omega$. The polarization, $\hat{\epsilon}_0$, of the incident light can be decomposed into a component $\hat{\epsilon}_p^0$, in the scattering plane (i.e., the plane formed by $\hat{\boldsymbol{s}}$ and $\hat{\boldsymbol{s}}_0$), and a perpendicular component $\hat{\epsilon}_s^0$. By means of analyzers, we detect two orthogonal components of the scattered light intensity, $I_\parallel$ having polarization $\hat{\epsilon}_a'$ and $I_\perp$ having perpendicular polarization $\hat{\epsilon}_a''$. The scattered intensity components are then given by

$$I_\parallel = \frac{1}{k^2r^2}\int_{\Delta\Omega} d\hat{\boldsymbol{s}} \int^{\Delta\Omega_0} d\hat{\boldsymbol{s}}_0\, I_0(\hat{\boldsymbol{s}}_0)|S_2(\hat{\boldsymbol{s}}_0,\hat{\boldsymbol{s}})\cdot\cos\phi\cos\phi_0 + S_1(\hat{\boldsymbol{s}}_0,\hat{\boldsymbol{s}})\sin\phi\sin\phi_0|^2 \tag{3a}$$

$$I_\perp = \frac{1}{k^2r^2}\int_{\Delta\Omega} d\hat{\boldsymbol{s}} \int^{\Delta\Omega_0} d\hat{\boldsymbol{s}}_0\, I_0(\hat{\boldsymbol{s}}_0)|S_2(\hat{\boldsymbol{s}}_0,\hat{\boldsymbol{s}})\cdot\cos\phi\sin\phi_0 - S_1(\hat{\boldsymbol{s}}_0,\hat{\boldsymbol{s}})\sin\phi\cos\phi_0|^2 \tag{3b}$$

with $\phi_0 = \cos^{-1}(\epsilon_p^0\cdot\hat{\epsilon}_0)$ and $\phi = \cos^{-1}(\hat{\epsilon}_a'\cdot\hat{\epsilon}_p)$. Here $\hat{\epsilon}_p$ is a unit vector along the polarization of the scattered light in the plane of scattering.

If the incident light is completely collimated $(\Delta\Omega_o = 0)$, light scattered directly backward $(\Delta\Omega = 0)$ will be polarized parallel to the incident light polarization. In this case, we can orient one of the analyzers parallel to the incident polarization direction $(\hat{\epsilon}_0 = \hat{\epsilon}_a')$. If the solid angles of the incident and collected light are sufficiently small and approximately equal, both $I_\parallel$ and $I_\perp$ will be present. However, the analyzer can still be positioned such that $(\hat{\epsilon}_0 \approx \hat{\epsilon}_a')$. Thus, in this case the collected light will still be highly polarized, and $I_\parallel \gg I_\perp$. For this case the expression for the residual intensity, $I_\parallel - I_\perp$, can be simplified as

$$I_\parallel - I_\perp \approx \frac{I_0}{k^2r^2}\int_\pi^{\pi-\vartheta_0} \mathrm{Re}(S_1^*(\vartheta)S_2(\vartheta))\sin\vartheta\, d\vartheta \tag{4}$$

with $\vartheta_0 = \sqrt{\Delta\Omega/\pi}$.

Consider a scattering medium such as mucosal tissue in which a thin layer of large scatterers $(d \gg \lambda)$ covers a highly turbid underlying tissue. Each of these layers gives rise to a different type of scattering. A small portion of the linearly polarized incident light will be backscattered by the particles in the upper layer. The rest of the signal diffuses into the underlying tissue and is depolarized by multiple scattering. This diffusive light, if not absorbed in the underlying tissue, returns to the surface. Thus the emerging light has two components, one from light back-scattered by particles of the first layer I_b and the other being diffusely reflected from the second layer I_d. I_b has a high degree of linear polarization that is parallel to the polarization of the incident light: $I_\parallel^b \gg I_\perp^b$. As a result of multiple scattering in the second layer, diffusely reflected light is mainly unpolarized, and $I_\parallel^d \approx I_\perp^d$. Therefore, the residual intensity of the emerging light $I_\parallel - I_\perp \approx I_\parallel^b - I_\perp^b$, is dominated by the contribution from the upper layer, and is mainly free from both absorption and scattering from the tissue below.

Expressions (3) or (4) relate $I_\parallel - I_\perp$ to the scattering amplitudes S_1 and S_2, which are functions of d, n, and the scattering wavelength $\lambda = 2\pi/k$. Therefore, the spectrum of the residual intensity varies with the scatterer's size and

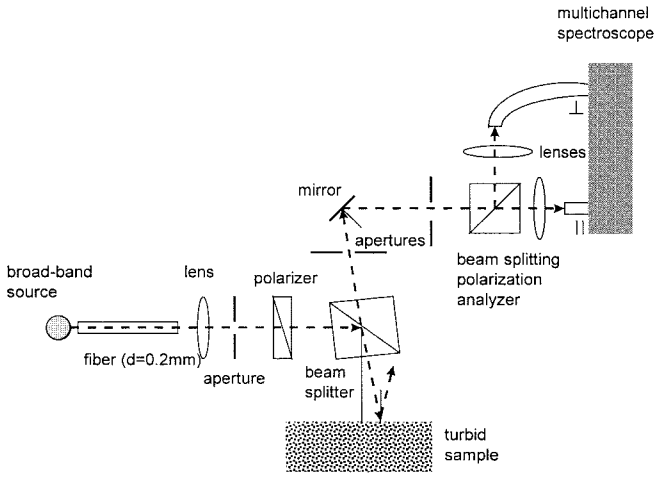

Fig. 1. Schematic diagram of polarization LSS system.

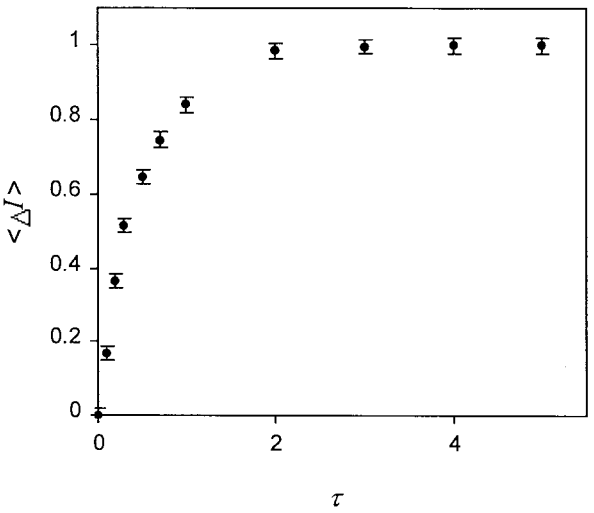

Fig. 2. Residual signal $\langle \Delta I \rangle$ from a single layer model averaged over 450–750-nm wavelength range measured for various values of optical thickness τ. $\langle \Delta I \rangle$ is normalized to one when $\tau \to \infty$.

relative refractive index. These quantities can thus be extracted by fitting the predictions of the Mie theory using (3) or (4) to the residual intensity spectrum.

III. Experimental Setup

To study the spectrum of polarized back-scattered light, we employ an instrument that delivers collimated polarized light on tissue and separates two orthogonal polarizations of back-scattered light. In our system (Fig. 1), light from a broadband source (250-W CW tungsten lamp) is collimated and then refocused with a small solid angle onto the sample, using lenses and an aperture. A broad-band polarizer linearly polarizes the incident beam. In order to avoid specular reflectance, the incident beam is oriented at an angle of $\sim$15° to the normal to the surface of the sample. The sample is illuminated by a circular spot of light of 2 mm in diameter. The reflected light is collected in a narrow cone ($\sim$0.015 rad), and two polarizations are separated by means of a broad-band polarizing beam splitter cube, which also serves as our analyzer. The output from this analyzer is delivered through 200-μm core diameter optical fibers into two channels of a multichannel spectroscope (quadruple spectroscope, Model SQ2000, Ocean Optics, Inc.). This enables the spectra of both components to be measured simultaneously in the range from 400 to 900 nm.

The beams are not perfectly collinear, and when they pass through the polarizer and analyzer cubes this gives rise to a small amount of distortion. Furthermore, the beamsplitter has different reflectivities for s and p polarizations. A diffusely reflective white surface was used as a standard to correct for wavelength nonuniformity, and to calibrate the signals in the two channels. $I_\perp(\lambda)$ and $I_{||}(\lambda)$ were each normalized to the corresponding background spectra, $I_{||}^B(\lambda)$ and $I_\perp^B(\lambda)$ taken with the white diffusing surface. This removed spectral nonuniformities in the light source. Thus, the experiments actually measured the normalized residual intensity $\Delta I = (I_{||}/I_{||}^B) - (I_\perp/I_\perp^B)$.

IV. Results

Our first experiments employed a single-layer physical model to simulate epithelium. The model consisted of polystyrene beads of diameters ranging from 0.5 to 10 μm to simulate cellular organelles (Polyscience, Inc), embedded in de-ionized water, glycol or glycerol. The thickness of these layers was varied so that the optical thickness $\tau = \mu_s z$ with μ_s the scattering coefficient and z the distance into the tissue ranged from 0.1 to 5. (A photon propagating through a medium with $\tau = 1$ will undergo one scattering event on average.) Large diameter polystyrene beads (d = 4–10 μm, refractive index $n_{\text{particle}} = 1.59$) were used to simulate cell nuclei. Since the relative refractive index of the beads in water, $n = n_{\text{particle}}/n_{\text{medium}} \sim 1.2$, is substantially higher than that of cell nuclei relative to cytoplasm, which is in the range $n = 1.03 - 1.1$ [12], some experiments used glycol ($n_{\text{medium}} = 1.45$) and glycerol ($n_{\text{medium}} = 1.48$) to decrease the relative refractive index of the beads, and therefore better approximate biological conditions.

We found that for $\tau \ll 1, I_{||}$ is almost 100 times larger than $I_\perp$.This demonstrates that single scattering from large spheroidal particles preserves polarization. As can be seen from Fig. 2, for the residual signal ΔI increases with τ. However, it saturates for values of $\tau > 1$. Because of the decollimation of the incident beam, the number of photons contributing to the residual signal decreases exponentially with optical depth. More than 85% of all polarized photons contributing to the residual signal are collected from an optical of 1, and 98% are collected from an optical depth of depth 2. This indicates that ΔI provides spectroscopic information about only the uppermost scatterers of a medium.

Our next experiments employed two-layer models. The upper layer consisted of polystyrene beads embedded in water, glycol or glycerol, as in the single layer experiments, with $\tau \sim 1$. The bottom layer was a gel containing mixtures of powdered $BaSO_4$ to provide scattering and human blood, the hemoglobin of which provided absorption. This physical model simulated human epithelial tissues. By adjusting the concentrations of the $BaSO_4$ and blood, the absorption and scattering properties could be made similar to those of biological tissue, since

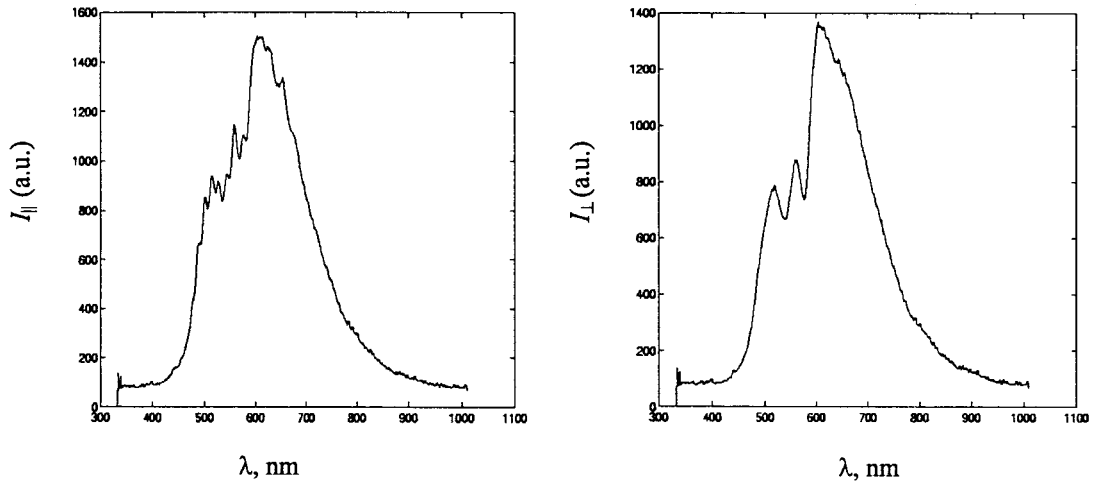

Fig. 3. Reflectance spectra of two-layer tissue model. The top layer consists of polystyrene beads in water, $d = 4.65\ \mu m, n = 1.19$. (a) Parallel polarization, (b) perpendicular polarization. Note the characteristic hemoglobin dips.

hemoglobin is known to be the major absorber in tissue in the optical spectral range [13]. The reduced scattering coefficient of the second layer μ_s' varied in the range from 2.0 to 3.0 mm^{-1}. The concentration of hemoglobin solution was approximately 200 mg/dl so that the corresponding absorption coefficient varied from 0.002 to 0.4 mm^{-1} in the wavelength region 450–780 nm.

Fig. 3 shows spectra of the $I_{||}$ and $I_{\perp}$ components of the reflected light from a two-layer model. In this experiment the top layer contained polystyrene beads with $d = 4.56$ μm, embedded in glycol. The standard deviation of their diameter, Δd, was 0.03 μm.[1] The optical thickness of the upper layer was $\tau \sim 0.85$. The bottom layer was optically thick, and its scattering and absorption properties were comparable to those of biological tissue [14]. As can be seen, strong hemoglobin absorption features are present in both $I_{||}$ and $I_{\perp}$. However, $I_{||}$ exhibits additional characteristic features due to backscattering by the beads in the upper layer. The residual spectrum, ΔI, is shown as the dashed line in Fig. 4(a). No hemoglobin absorption features are present, and the diffusive background from the lower layer is completely removed. The ripple structure [15] characteristic of scattering from spheres is now clearly apparent. The predictions of Mie theory for scatterers with $d = 4.56$ μm, $\Delta d = 0.03$ μm, and $n = 1.19$ are in good agreement with experiment (solid line). The residual spectra obtained in experiments with other bead diameters (5.7, 8.9, and 9.5 μm), embedded in any of the media used (water, glycol, and glycerol) had no measurable diffusive background component, and also agreed with Mie theory predictions. Fig. 4(b) shows theory and experiment for the 9.5 μm beads. The results for 8.9- and 5.7-μm diameter beads in glycerol and glycol are shown in Fig .4(c) and (d), respectively. Again, there is good agreement between experiment and theory. One can clearly see that the high frequency ripple structure decreases as the relative refractive index gets smaller. However, the low frequency oscillations are still clearly seen. Small disagreements between theory and experiment may have resulted from imperfect calibration of the instrument for the wavelength dependence of the optical elements used.

We then performed experiments with cell monolayers (Fig. 5). As before, a thick layer of gel containing $BaSO_4$ and blood was placed underneath to simulate underlying tissue. Three types of cells were prepared as described: isolated normal intestinal epithelial cells [16], intestinal epithelial T84 intestinal malignant cell line [17], and Chinese hamster ovary (CHO) fibroblasts [18]. The setup was similar to the experiments with beads. The cell nuclei however, had relative refractive indexes smaller then those of beads, as well as larger size distributions, which almost completely eliminates the ripple structure. The predictions of Mie theory were fit to the observed residual spectra. The fitting procedure used three parameters, average size of the nucleus, standard deviation in size (a Gaussian size distribution was assumed), and relative refractive index.

For normal intestinal epithelial cells, the best fit was obtained using $d = 5.0$ μm, $\Delta d = 0.5$ μm, and $n = 1.035$ [Fig. 6(a)]. For CHO fibroblasts, we obtained $d = 7.0$ μm, $\Delta d = 1.0$ μm, and $n = 1.051$ (data not shown). For T84 intestinal malignant cells the corresponding values were $d = 9.8$ μm, $\Delta d = 1.5$ μm, and $n = 1.04$ [Fig 6(b)].

In order to check these results, the distribution of the average size of the cell nuclei was measured by morphometry on identical cell preparations that were processed in parallel for light microscopy (Fig. 5). The nuclear sizes and their standard deviations were found to be in very good agreement with the parameters extracted from Mie theory. A histogram showing the size distributions obtained for the normal intestinal epithelial cells and T84 cells are shown in Fig. 7. The accuracy of the average size is estimated to be 0.1 μm, and the accuracy in n as 0.001. Note the larger value of n obtained for T84 intestinal malignant cells, which is in agreement with the hyperchromaticity of cancer cell nuclei observed in conventional histopathology of stained tissue sections.

[1]The values of the standard deviation in diameters of the polystyrene beads were obtained from the spectral transmission curves using a broad-band source.

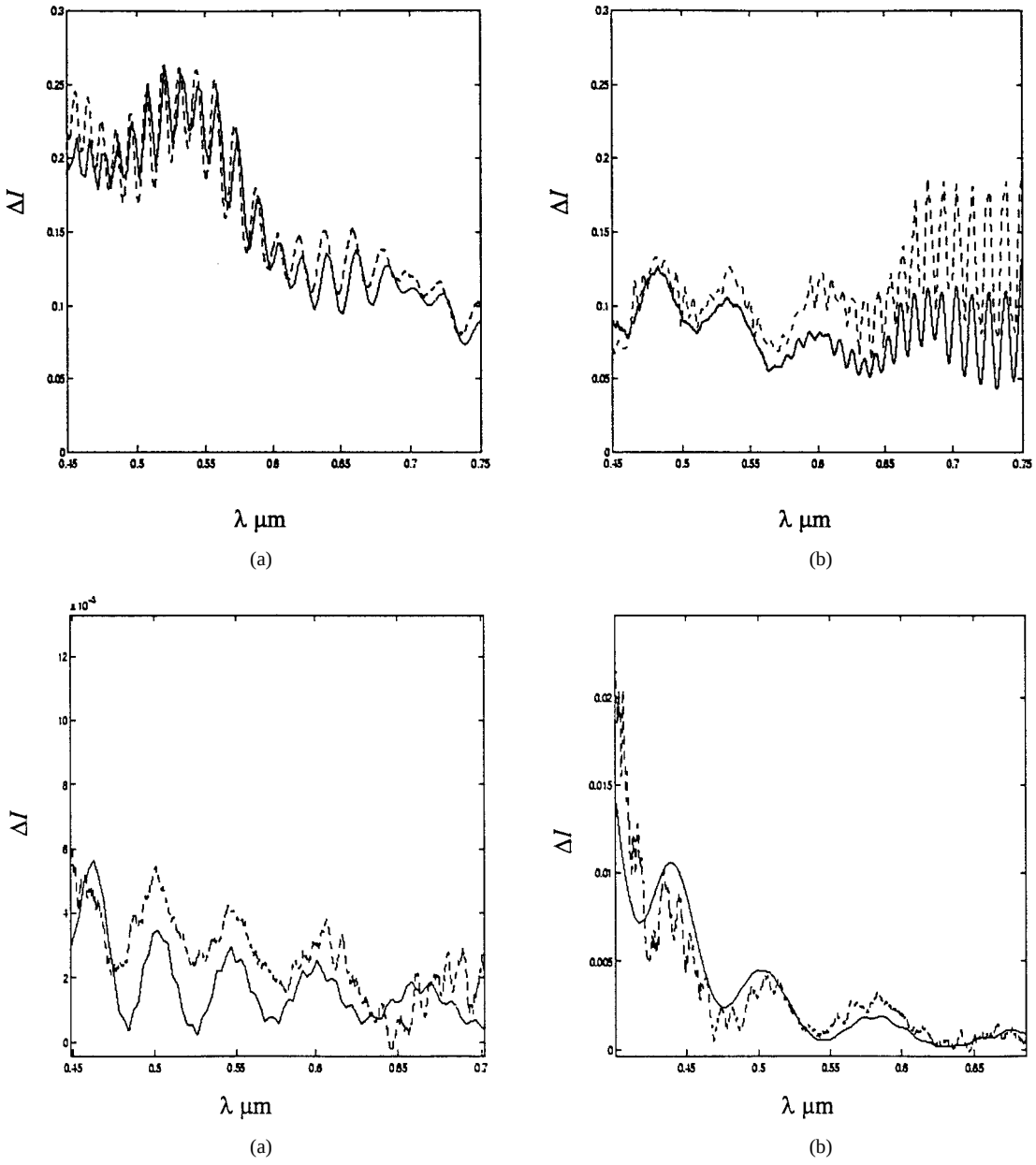

Fig. 4. Spectra of polarized (residual) component of backscattered light from two-layered tissue model. Top layer: (a) $d = 4.65$-μm beads in water, $n = 1.19$; (b) $d = 9.5$-μm beads in water ($n = 1.19$); (c) $d = 8.9$-μm beads in glycol ($n = 1.07$); (d) $d = 5.7$-μm beads in glycerol ($n = 1.09$). The data (dashed lines) are in good agreement with Mie calculations (solid lines). Absorption features of hemoglobin are completely removed.

We performed studies with *ex vivo* normal and tumorous human colon tissue samples obtained immediately after surgical resection. Fig. 8 shows the residual spectra. As can be seen, the spectral features are similar to the corresponding spectra obtained in the experiments with the normal colon cell and T84 colon tumor cell monolayers (Fig. 6). Fig. 9 shows the size distributions obtained for the normal and the cancerous tissues by fitting the Mie theory to the data. For the normal tissue, the best fit was obtained using $d = 4.8$ μm, $\Delta d = 0.4$ μm, and $n = 1.035$. For the tumorous tissue the corresponding values were $d = 9.75$ μm, $\Delta d = 1.5$ μm, and $n = 1.045$. The analysis clearly differentiates the normal and tumourous tissues. The relative increase in the nuclear refractive index from normal to cancerous tissue is also consistent with those of the cell monolayers.

V. Discussion

The experiments reported here show that polarization LSS is capable of extracting morphological information from living cells in the presence of the large background from underlying tissue. The size distributions for monolayers were compared to light microscopy and found to be in good agreement with all three cell lines studied. The accuracy of the values extracted for both size and standard deviation was approximately 0.1 μm, which makes the method useful in differentiating cell nuclei of different cell types, including cancerous and noncancerous cells of the same organ. The ability to detect nuclear enlargement and changes in refractive index, which can be related to the amount of DNA and protein in the nucleus, has potentially valuable clinical applications.

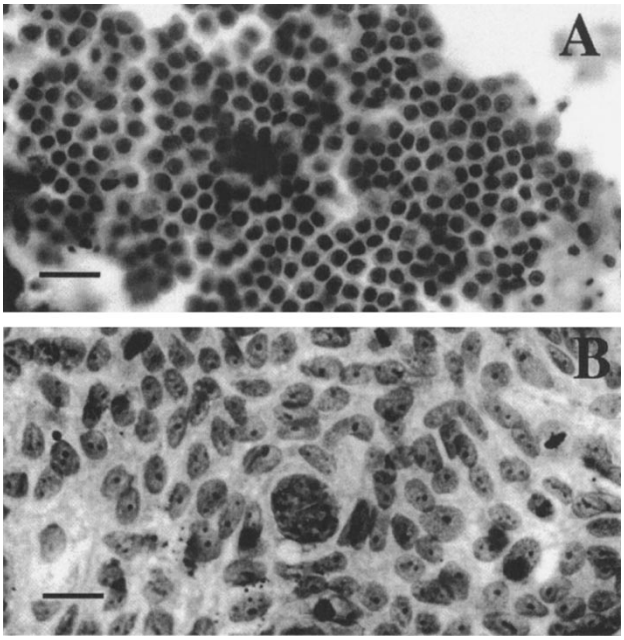

Fig. 5. Microphotograph of the isolated normal intestinal epithelial cells (panel A) and intestinal malignant cell line T84 (Panel B). Note the uniform nuclear size distribution of the normal epithelial cell (A) in contrast to the T84 malignant cell line which at the same magnification shows a larger nuclei and more variation in nuclear size (B). Solid bars equals 20 μm in each panel.

Because the relative refractive index of cell organelles is small and the epithelial layer is thin, the signal from the cellular layer is weak compared to the background from the underlying tissue. Extracting signatures of the cellular structures thus requires finding a small signal in a large background. However, as seen in Fig. 4, the residual spectrum, obtained by subtracting the parallel and perpendicular components of the reflectance from polarized incident light, effectively removes both the diffuse background and spectral distortions due to absorption. This should be contrasted with our earlier approach in which reflectance from unpolarized incident light was studied, and a model based on diffusion theory was then used to remove the effects due to hemoglobin absorption and scattering from the underlying tissue [3]. The resulting signal could then be analyzed to extract information about the structures in the epithelial tissue layer.

The new approach is not constrained by the limitations of a model, other than the assumption that the light backscattered by the cells in the epithelial layer retains the polarization of the incident light. Multiple scattering events randomize the polarization, enabling removal of the background simply by subtracting the two orthogonal polarization components. Generally, the signals seen in the monolayers have a very pronounced polarization content, of the order of 1%–10%, depending on the relative refractive index and the size of the particles.

As seen in Fig. 6, Mie theory can be used to accurately describe the residual spectra of the epithelial cell layer. Furthermore, Fig. 7 establishes that the resulting morphological information is in good agreement with the directly measured distributions. This shows that Mie theory provides an adequate method for extracting information about cell nuclei. Mie theory was used to analyze the backscattered signal by varying the

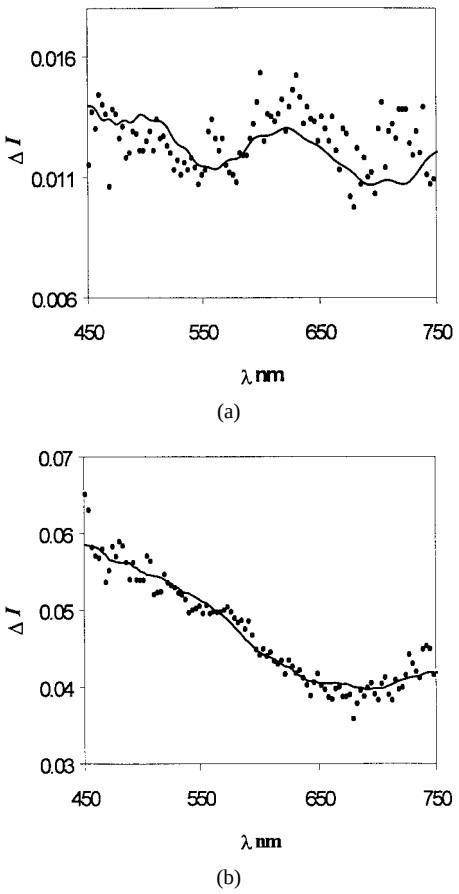

Fig. 6. Spectrum of polarized component of backscattered light from (a) normal intestinal cells, (b) T84 intestinal malignant cells. A monolayer of cells was placed on top a gel containing hemoglobin and barium sulfate. Dashed line: experimental data. Solid line: Mie theory fit. See text for details.

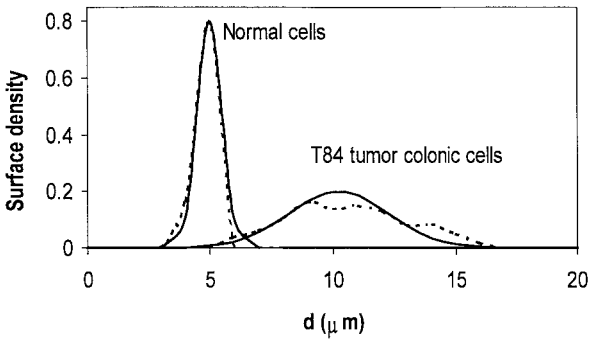

Fig. 7. Nuclear size distributions for T84 intestinal malignant cells and normal intestinal cells. In each case, the solid line is the distribution extracted from the data and the dashed line is the distribution measured using light microscopy.

average nuclear size d, the standard deviation in size Δd, and the relative refractive index n. We found that good agreement could be achieved only for a single set of parameters. Interestingly, in the rigorous Mie theory, the dependence on d and n does not always enter as the product $(n-1)d$. Thus, the residual experimental spectra contain sufficient information to extract d and n independently.

As pointed out in [2] and [3], elastic scattering by cells is due to a variety of cellular organelles, including mitochondria, a variety of endosomes and other cytoplasmic vesicles, nucleoli, and nuclei. The smaller organelles are responsible for large

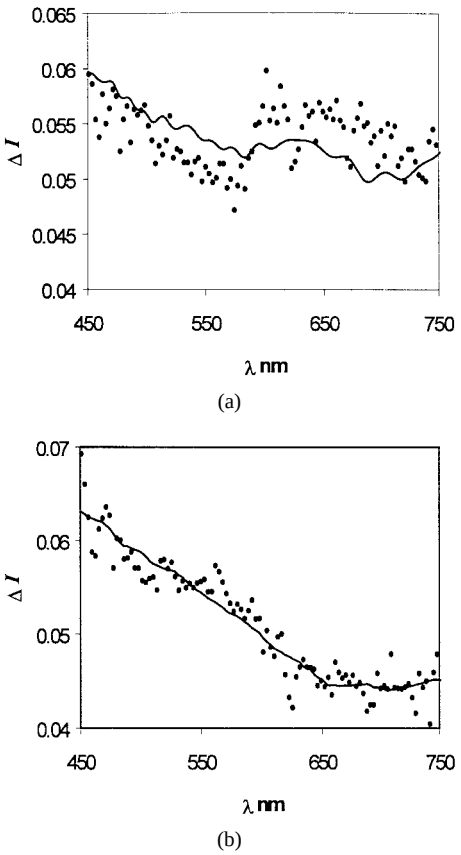

Fig. 8. Spectrum of polarized component of backscattered light from (a) normal human colon tissue and (b) tumorous colon tissue. Dashed line: Experimental data. Solid line: Mie theory fit.

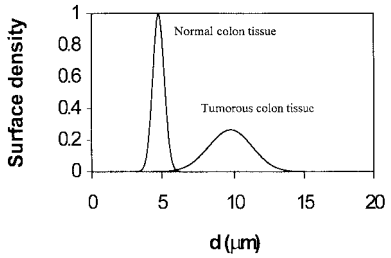

Fig. 9. Nuclear size distributions extracted from the data measured from the normal and tumorous colon tissues.

angle scattering, whereas the nucleus contributes to scattering at small angles. Our experiments confirm that the variation in backscattering as a function of wavelength is mainly associated with scattering by nuclei, as well. By changing the angle of collection, it may be possible to study the structure of other cellular organelles.

This new method of extracting information about cellular structure can be compared with existing methods such as flow cytometry, morphometry, ploidy analysis and confocal microscopy [19]–[21]. Except for confocal microscopy, these other techniques are essentially *in vitro* and necessitate tissue removal. In flow cytometry, cells suspended in a fluid are ejected from a nozzle and made to flow, and are then sorted using laser light according to size and shape, using angular light scattering properties or fluorescence from attached flurophores. Histology and morphometry require tissue removal, processing, and microscopic examination to reveal morphological characteristics. Whereas LSS provides average information over a population of typically 1000–10 000 cells, microscopy studies a limited number of individual cells, which provides valuable information. However, processing information about individual cells is time consuming, especially if it is desired to sample a large surface area and search for structural abnormalities. Confocal microscopy has not reached the resolution needed to estimate the size of small cellular structures.

Polarized LSS can be implemented *in situ* without the need for tissue preparation or removal. Fitting the data to Mie theory gives an accurate quantitative estimate of the size distributions of cell nuclei. Moreover, it provides additional information about relative refractive index of cell organelles, which is very difficult to obtain using existing methods, and which can be valuable inasmuch as the refractive index of the nucleus is related to the concentration of nucleic acids, an important neoplastic indicator.

VI. Conclusion

The results reported here indicate the potential and promise of polarization LSS for clinical studies. Based on the initial studies reported here, a polarized LSS instrument is being developed for clinical use in which light delivery and collection is accomplished by means of optical fibers. The fiber probe can be inserted in the endoscope biopsy channel or any similar device, depending on the type of the procedure and the organ under study. Polarizer and analyzer can be placed at the tip of the probe in front of the delivery and collection fibers. This instrument will be used during endoscopic or similar procedures to detect precancerous changes in vivo in real time.

Acknowledgment

The T84 cells were generously provided by Dr. W. Lencer, Children's Hospital. This work was carried out at the MIT Laser Biomedical Research Center.

References

[1] A. Brunsting, and P. Mullaney, "Differential light scattering from spherical mammalian cells," *Biophys. J.* vol. 14, pp. 439–453, 1974.
[2] J. Mourant, J. Freyer, A. Heilscher, A. Eick, D. Shen, and T. Johnson, "Mechanisms of light scattering from biological cells relevant to noninvasive optical-tissue diagnosis," *Appl. Opt.* vol. 37, pp. 3586–3593, 1998.
[3] L. T. Perelman, V. Backman, M. Wallace, G. Zonios, R. Manoharan, A. Nusrat, S. Shields, M. Seiler, C. Lima, T. Hamano, I. Itzkan, J. Van Dam, J. M. Crawford, and M. S. Feld, "Observation of periodic fine structure in reflectance from biological tissue: A new technique for measuring nuclear size distribution," *Phys. Rev. Lett.*, vol. 80, pp. 627–630, 1998.
[4] R. S. Cotran, S. L. Robbins, and V. Kumar, *Robbins Pathological Basis of Disease*. Philadelphia, PA: W. B. Saunders, 1994.
[5] R. Riddell, H. Goldman, D. Ransohoff, H. D. Appelman, C. M. Fenoglio, R. C. Haggitt, C. Ahren, P. Correa, S. R. Hamilton, B. C. Morson, S. C. Sommers, and J. H. Yardley, "Dysplasia in inflammatory bowel-disease, standardized classification with provisional clinical-applications," *Human Pathol.*, vol. 14, pp. 931–968, 1983.
[6] J. R. Mourant, I. J. Bigio, J. Boyer, R. L. Conn, T. Johnson, and T. Shimada, "Spectroscopic diagnosis of blader cancer with elastic light scattering," *Laser Surg. Med.*, vol. 17, pp. 350–357, 1995.
[7] S. G. Demos and R. R. Alfano, "Temporal gating in highly scattering media by the degree of optical polarization," *Opt. Lett.*, vol. 21 no. 2, pp. 161–163, 1996.
[8] K. M. Yoo and R. R. Alfano, "Time resolved depolarization of multiple backscattered light from random media," *Phys. Lett. A*, vol. 142, pp. 531–536, 1989.

[9] R. R. Anderson, "Polarized light examination and photography of the skin," *Arch. Dermatol.* vol. 127, pp. 1000–1005, 1991.
[10] S. J. Demos, R. R. Alfano, "Optical polarized imaging," *Appl. Opt.* vol. 36, pp. 150–155, 1997.
[11] C. F. Bohren and D. R. Huffman, *Absorption and Scattering of Light by Small Particles*. New York: Wiley, 1983.
[12] B. Beauvoit, T. Kitai, and B. Chance, "Contribution of the mitochondrial compartment to the optical properties of rat liver: a theoretical and practical approach," *Biophys. J.*, vol. 67, pp. 2501–2510, 1994.
[13] A. G. Yodh and B. Chance, "Spectroscopy and imaging with diffusion light," *Phys. Today*, vol. 48, no. 3, pp. 34–40, 1995.
[14] G. I. Zonios, R. M. Cothren, J. T. Arendt, J. Wu, J. Van Dam, J. M. Crawford, R. Manoharan, and M. S. Feld, "Morphological model of human colon tissue fluorescence," *IEEE Trans. Biomed. Eng.*, vol. 43, pp. 1–10, 1996.
[15] Van de Hulst, *Light Scattering by Small Particles*. New York: Dover, 1957).
[16] R. S. Blumberg, C. Terhost, P. Bleicher, F. V. McDermott, C H Allan, S B Landau, J S Trier, S. P. Balk, "Expression of a nonpolymorphic MHC class I-like molecule, CDID, by human intestinal epithelial cells," *J. Immunol.*, vol. 147, pp. 2518–2524, 1991.
[17] K. Dharmsathaphorn and J. L. Madara, "Eastablished intestinal cell lines as model systems for electrolyte transport studies,'' *Methods Enzymol.*, vol. 192, pp. 354–389, 1990.
[18] R. I. Freshney, *Animal Cell Culture: A Practical Approach*, 2nd ed. Oxford, U.K.: IRL, 1992.
[19] A. V. Chernyshev, V. I. Prots, A. A. Doroshkin, and V. P. Maltser, "Measurement of scattering properties of individual particles with a scanning flow cytometer," *Appl. Opt.*, vol. 34, pp. 6301–6309, 1995.
[20] J. P. A. Baak and J. Oort, *A manual of morphometry in diagnostic pathology*. New York: Springer Verlag, 1983.
[21] S. W. Paddock, Ed., "Confocal microscopy methods and protocols," in *Methods in Molecular Biology*. Totowa, NJ: Humana, 1999, p. 122.

Vadim Backman was born in St. Petersburg (former Leningrad), Russia, in 1973. He received the M.S. degree from Leningrad Polytechnic Institute in 1996, and M.S. degree in physics from Massachusetts Institute of Technology, Cambridge, MA, in 1998. He is currently pursuing the Ph.D. degree in medical engineering and medical physics from the Harvard University–M.I.T. Division of Health Sciences and Technology.

From 1993 to 1996, he was a Research Assistant in the Laboratory for Laser Polarization Spectroscopy at the Ioffe Physico-Technical Institute, St. Petersburg, where he worked in the theory of the polarization effects in light-molecule interactions. He joined the MIT George R. Harrison Spectroscopy Laboratory, Cambridge, MA, in 1996, and has been studying tissue light scattering spectroscopy as a tool in medicine. His interests include the use of spectroscopy for the detection of precancerous changes *in vivo*, development of the theoretical approaches to describe light propagation in biological media, and biomedical instrumentation.

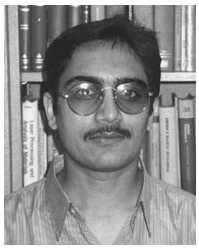

Rajan Gurjar received the B.Tech. degree in engineering physics from the Indian Institute of Technology (I.I.T.), Bombay, India, and the Ph.D. degree from I.I.T., Kanpur, in March 1998.

His specialization is in the field of experimental atomic physics and nonlinear optics. Immediately after his doctorate he joined George R. Harrison Spectroscopy Laboratory at the Massachusetts Institute of Technology, Cambridge, as a Post-Doctoral Fellow and is engaged in various biomedical projects exploring the light tissue interaction using polarized light scattering techniques. He is also engaged in a collaborative project with the department of Toxicology to study fluorescence from various DNA-Protein adducts.

Kamran Badizadegan received the B.S. degree in chemical engineering from the Massachusetts Institute of Technology, Cambridge, in 1988, and the M.D. degree from Harvard Medical School, Cambridge, MA, in 1993.

Subsequently, he completed a residency in anatomic pathology at the Brigham and Women's Hospital and a fellowship in pediatric pathology at the Children's Hospital, both in Boston, MA. He is a Staff Pathologist at the Children's Hospital, a consulting pathologist at the Brigham and Women's Hospital, and an Instructor in Pathology at the Harvard Medical School. His current clinical practice and research are focused on gastrointestinal and liver pathology, and he is actively involved in teaching the same at the Harvard Medical School. His basic research involves the physiology and cellular biology of model and native intestinal epithelia.

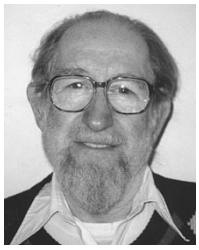

Irving Itzkan received a Bachelor degree in engineering physics from Cornell University, Ithaca, NY, in 1952, a Masters degree in electrical engineering from Columbia University, New York, NY, in 1961, and the Ph.D. degree in physics from New York University, New York, NY, in 1969.

He has been a Senior Scientist in the the Massachusetts Institute of Technology Laser Biomedical Research Center, Cambridge, MA, since 1988. From 1956 to 1969, he was with Sperry Rand and from 1969 to 1985, with the Avco–Everett Research Laboratory where he worked on many different aspects of laser research. His principal present research interest involves using optical spectroscopy to diagnose disease.

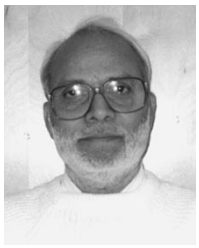

Ramachandra R. Dasari received the M.Sc. degree from Benaras Hindu University in 1956 and Ph.D. degree in physics from Alighar Muslim University in 1960.

He was Professor of Physics at Indian Institute of Technology, Kanpur, until 1978 and worked at the National Research Council, Ottawa, Canada, and University of British Columbia before joining the Massachusetts Institute of Technology, Cambridge, MA, in 1980. His current research interests include cavity QED and single atom laser characteristics and laser spectroscopy of biological tissue and ultrasensitive detection of carcinogenic protein adducts.

Lev T. Perelman received the M.S. degree from the Department of Physics at the Belorussian University in 1982 and Ph.D. degree in physics from Institute of Physics, Minsk, Russia, in 1989.

He joined the Massachusetts Institute of Technology, Cambridge, MA, in 1992, where he currently holds a Principal Research Scientist appointment at George R. Harrison Spectroscopy Laboratory. His research interests are in the field of medical applications of optics and spectroscopy. His current projects include minimally invasive detection of precancerous condition in human epithelial tissues with light scattering spectroscopy and optical imaging of tissue.

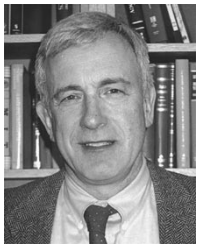

Michael S. Feld received the S.B. degree in physics and the S.M. degree in humanities and sciences in 1963, and the Ph.D. degree in physics in 1967, all from the Massachusetts Institute of Technology, Cambridge, MA.

He is a Professor of Physics at the Massachusetts Institute Of Technology and directs the George R. Harrison Spectroscopy Laboratory there. He conducts research in biological physics and spectroscopy. He is also active in laser physics, particularly the coherent interaction of light with atomic and molecular systems, where his interests include cavity quantum electrodynamics, superradiance, and laser-nuclear physics. His publications include both theoretical and experimental topics. He has also done research in the history of science.